Airy beams propagation in optically induced photonic lattices

Bojana Bokić*[a], Falko Diebel[b], Dejan Timotijević[a], Aleksandra Piper[a], Martin Boguslawski[b], Dragana Jović[a] and Cornelia Denz[b]

[a]Institute of Physics, University of Belgrade, P.O. Box 68, 11001 Belgrade, Serbia;
[b]Institut für Angewandte Physik and Center for Nonlinear Science (CeNoS), Westfälische Wilhelms-Universität Münster, 48149 Münster, Germany

Abstract

We show both experimentally and numerically, control over the acceleration of two-dimensional Airy beam propagating in optically induced photonic lattice. Varying the lattice strength and including various defects we can reach a state, where the acceleration is completely stopped. We find an additional class of discrete lattice beams, localized and defect modes observed with Airy beams propagating in diamond optically induced photonic lattice.

Keywords: accelerating beams, photonic lattices, defects

1. INTRODUCTION

Airy beams are a well-known type of accelerating optical beams [1]. Unlike ordinary optical wave fields, Airy beams show an accelerated transverse intensity distribution which remains invariant along their parabolic trajectories [2]. Originally, Airy beams were introduced as wave functions solving the one-dimensional Schrödinger equation for free particles. Due to the equivalence between the Schrödinger equation in quantum mechanics and the paraxial equation of diffraction in optics these concepts can be transferred to optics. The ballistic-like properties of Airy beams qualify them for various applications ranging from particle trapping along curved paths [3] and self-bending plasma channels [4] to ultrafast self-accelerating pulses [5] and Airy light bullets accelerating in both transverse dimensions and in time [6]. Over the years, two-dimensional Airy beams have been systematically investigated, particularly in the field of optics and atom physics. In terms of experimental realization, optics provides a fertile ground to directly observe and study the properties of such non-spreading waves in detail. One of the features of these beams is their potential for applications in nonlinear optics: nonlinear interaction of light with some material and a study of accelerating beam dynamics inside nonlinear media. Formation of accelerating self-trapped optical beams has been proposed employing the different self-focusing nonlinearities, ranging from Kerr to quadratic nonlinearities, and also using an optically induced refractive-index potential [7, 8].

The key for the realization of all-optical guiding and switching architectures is control of the propagating light with light itself. Propagation dynamics of light is dramatically changed with the presence of photonic lattice. Recently, defect guiding Airy beams in optically induced waveguide arrays is studied [9]. The propagation of such accelerated beams inside a two-dimensional optically induced photonic lattice has not been observed yet.

We analyze theoretically and experimentally how an optically induced photonic lattice affects and modifies acceleration of Airy beams. Various conditions for the propagation and preservation of the Airy beam shape are considered. The acceleration of Airy beams is controlled by varying the lattice strength (refractive index modulation) and by introducing positive and negative single-side defects. We find that a modification of refractive index modulation leads to reduced Airy beam acceleration and formation of discrete lattice beams. However, inclusion of lattice defects changes the beam dynamics completely: with the negative defect Airy beams experience a strong repulsion, while in the presence of positive defect they form localized defect modes.

*bojana@ipb.ac.rs; phone +381 11 3713161; fax +381 113162190

Nonlinear Optics and Its Applications VIII; and Quantum Optics III, edited by Benjamin J. Eggleton, Alexander L. Gaeta, Neil G. R. Broderick, Alexander V. Sergienko, Arno Rauschenbeutel, Thomas Durt, Proc. of SPIE Vol. 9136, 91360S · © 2014 SPIE · CCC code: 0277-786X/14/$18 · doi: 10.1117/12.2052272

2. THEORETICAL BACKGROUND AND EXPERIMENT

To study the propagation behavior of Airy beams in optical systems with induced photonic lattice, we start with considering the following scaled paraxial equation of diffraction for electric field Ψ

$$i\partial_\zeta \Psi + \frac{1}{2}(\partial_\chi^2 \Psi + \partial_\nu^2 \Psi) + \frac{1}{2} k_0^2 w_0^2 \Delta n^2 (\mathrm{I}_{indu}) \Psi = 0 \quad . \tag{1}$$

Here, $\chi=x/w_0$ and $\nu=y/w_0$ are dimensionless transverse coordinates scaled by the characteristic length w_0. $\zeta=z/kw_0^2$ represents the dimensionless propagation distance with $k=2\pi n/\lambda$. The photonic lattice enters this equation in terms of an intensity-dependent refractive index modulation Δn^2 (I_{indu}), which represents the optical induction process. This equation is also suitable to cover nonlinear light propagation in the case the inducting intensity becomes a function of field Ψ itself. In this contribution, however, we restrict ourselves to linear effects.

Considering the case for light propagation in homogenous, linear medium, where $\Delta n^2=0$ holds, the wave equation (1) can always be separated into two parts, each depending only on one transverse coordinate χ or ν, respectively. Therefore, the solution Ψ is also separated and can be written as a product in the following form: $\Psi(\chi,\nu,\zeta)=\Psi_1(\chi,\zeta)\Psi_2(\nu,\zeta)$. As firstly shown in [1] each part of the wave equation is fulfilled by a non-dispersive Airy solution. Thus, the overall solution of Eq. (1) reads as:

$$\Psi(\chi,\nu,\zeta) = \prod_{X=\{\chi,\nu\}} Ai(\mathrm{X} - (\zeta/2)^2) \exp(\mathrm{i}(\mathrm{X}\zeta/2) - \mathrm{i}(\zeta^3/12)) \quad . \tag{2}$$

We have to consider truncated solution with finite extent and energy, like $\Psi_\chi(\chi,0)=\mathrm{Ai}(\chi)\exp(a_\chi\chi)$, with the positive decay length a_χ, typically $a_\chi<<1$. It has been shown, that this kind of solution still solves the wave equation [1] and the distinguished properties of Airy beams are preserved. Although, the transverse intensity pattern is now non-spreading over a limited propagation distance, this easily covers the longitudinal range necessary to observe sufficient transverse displacement of the truncated Airy beams.

Our experimental setup for all measurements is sketched in Fig. 1(a). We use the beam from frequency-doubled, continuous wave laser ($Nd:YVO_4$) emitting at λ = 532 nm. The beam is split into two partial beams, each illuminating a high-resolution, programmable, phase-only spatial light modulator (SLM1, SLM2). The first one (SLM1), in combination with two lens and Fourier mask, is employed for making of nondiffracting induction beam. By using the calculated phase patterns, addressed to spatial light modulators, we modulate the phase and amplitude of incident plane wave and thereby obtain the complex field of desired nondiffracting induction beam. This modulated beam is then sent through the 20 mm long $Sr_{0.60}Ba_{0.40}Nb_2O_6$ (SBN:Ce) photorefractive crystal, externally biased with $E_{ext}\approx$2000 V/cm, an electric dc field. The induction beam is set to be ordinarily polarized with respect to the crystal's optical axis, to minimize the feedback of the written refractive index structure onto the induction beam itself. Because of the high polarization anisotropy of electro-optic coefficients of SBN:Ce crystal we are able to induce sufficient refractive index modulations to affect the propagation of extraordinarily polarized Airy beam. The Airy beam is made the same way as the nondiffracting induction beam by means of the second modulator (SLM2) and the encoded complex field, calculated in real space with the Eq. (2). To accurately overlay two beams in the crystal, we place a beam splitter directly in front of the SBN crystal. In addition, by illuminating the crystal homogeneously with white light, we can erase modulations of the written refractive index. With an imaging lens and a camera, mounted on a translation stage, we record the intensity distribution in different transverse planes.

The propagation characteristics of 2D Airy beam propagating in a homogeneous medium are shown experimentally in Fig. 1. The intensity distributions at the front and back face of the SBN:Ce crystal are shown in Fig. 1(b) and 1(c), respectively. To experimentally realize the photonic lattice which should control the propagation trajectory of Airy beam we use the technique of optical induction [10, 11]. Figure 1(d) shows the recorded intensity distribution of experimentally realized nondiffracting beam used to optically induce a two-dimensional square lattice. The lattice period $\Lambda=\pi/k_t\approx$25μm is chosen to match exactly the distance between the main and the first neighboring lobes of Airy beam.

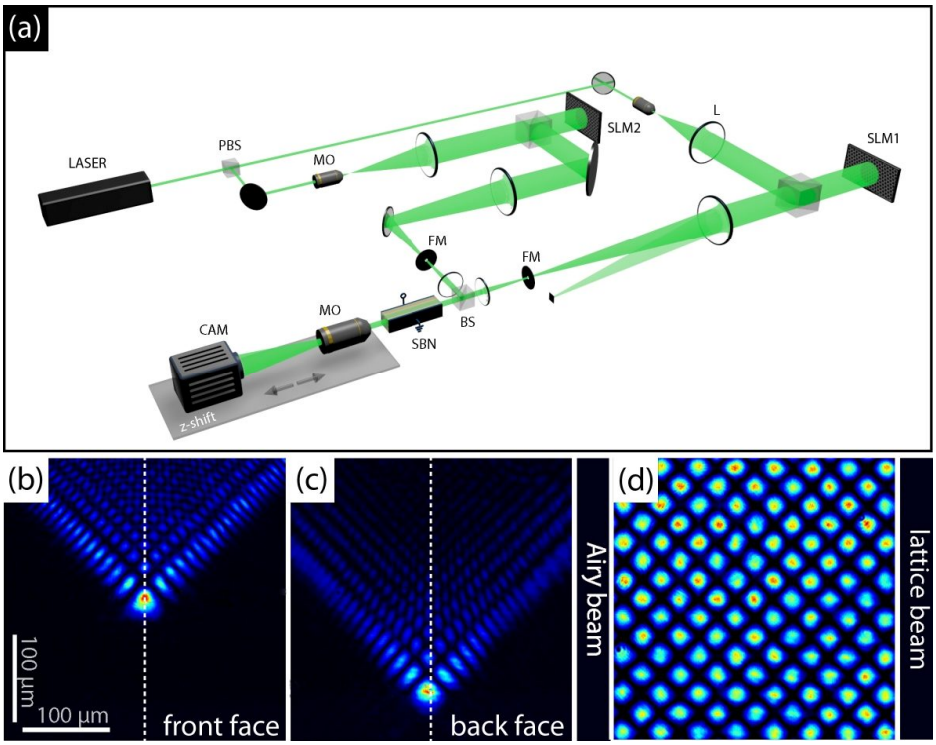

Figure 1. Experimental realization of two-dimensional Airy beams and photonic lattices. (a) Experimental setup. LASER: Nd:YVO_4 at λ = 532 nm, (P)BS: (polarizing) beam splitter, FM: Fourier mask, L: lens, MO: microscope objective, SBN: strontium barium niobate crystal, SLM1, SLM2: spatial light modulators. (b) Experimentally recorded intensity distribution of the Airy beam at the front face and (c) intensity distribution at the back face. (d) Lattice intensity distribution of the induced refractive index modulation.

We support our experiments with comprehensive numerical simulations by solving the paraxial wave equation (1), which models the light propagation in media with inhomogeneous refractive index modulations. The process of optical induction into a photorefractive material like SBN is represented by $\Delta n^2(I_{indu})$, which can be calculated in the full anisotropic model with a relaxation method. Since only linear effects are considered, the inducing intensity I_{indu} is solely given by the intensity of nondiffracting beam, $I_{indu}=|E_{ndB}|^2$ (cf. Eq. (3)). Even though the paraxial wave equation stays in the linear regime, it is not solvable analytically and we need to rely on proven beam propagation methods. The propagation equation (1) is solved numerically, using a split-step Fourier method described earlier in [12, 13].

3. CONTROL OF AIRY BEAM SELF-ACCELERATION WITH PHOTONIC LATTICES

Here, we observe the way that optically induced photonic lattice affects the acceleration of two-dimensional Airy beams. We have the self-bending of Airy beams on one side and the waveguiding and discrete diffraction effects of the photonic lattice on the other. By increasing the modulation of refractive index we affect the beam's acceleration and by increasing the lattice strength we affect the slowing down of the beam until we make it stops for a certain value.

In our investigation of propagation behavior of two-dimensional Airy beams in a regular photonic lattice, we are observing the influence of defect lattices as well. We consider single-site defect lattices with positive and negative variable defect strength.

Defect lattices are realized using the nondiffracting zero-order Bessel beam. We are increasing or decreasing the modulation of refractive index thus making a different defect lattices. We use the effective intensity distribution of incoherent superposition of two nondiffracting beams, the lattice beam and the Bessel beam, and make two-dimensional

defect lattice. Since we have incoherent superposition of the two nondiffracting beams we don't need to take care about the phase relation between them and potential unwanted intensity modulation in longitudinal direction. As shown earlier, this multiplexing method is suitable for fabrication of a whole set of different two-dimensional super and defect lattices, including negative defects [14]. For the realization of negative defect we apply the electric dc field, anti-parallel to the optical c-axis and obtain defocusing nonlinearity at the site where the Bessel beam is set to propagate.

Figure 2 illustrates the basic scheme of defect realization. The regular lattice is made by the intensity distribution shown in Fig. 2(a). Afterwards, the Bessel beam (Fig. 2(b)), illuminates the crystal and depending on the direction of applied electric field, the refractive index at one particular site gets increased or decreased. The resulting effective intensity distributions for the positive and negative defect lattices are shown in Fig. 2(c) and Fig. 2(d), respectively. Figures 2(e) and 2(f) show the numerically calculated refractive modulations for both defect lattices.

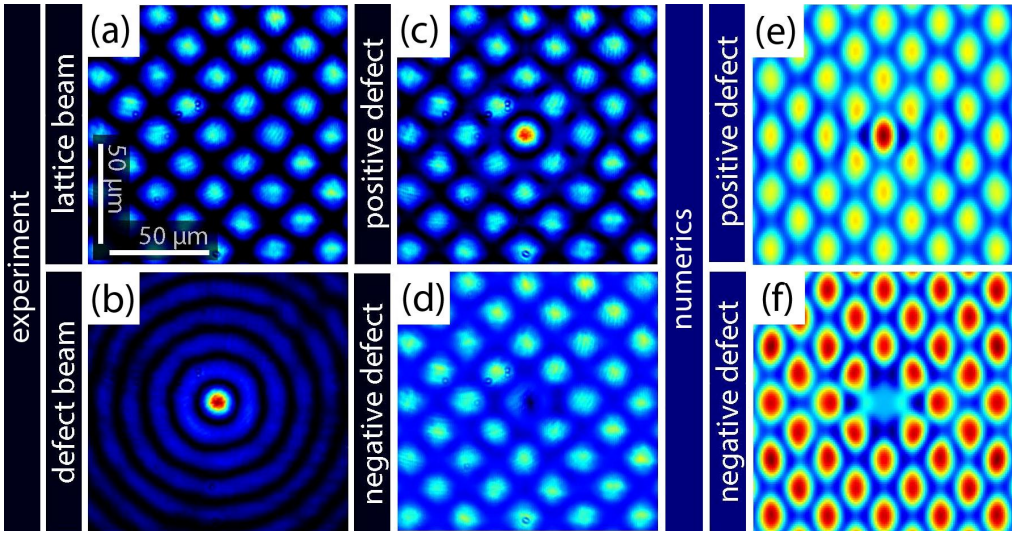

Figure 2. Defect generation in optically induced photonic lattice. (a) Experimental realization of the diamond lattice, (b) the Bessel beam, (c) the positive defect lattice and (d) the negative defect lattice. (e) Numerical realization of the positive and (f) negative lattice defects.

Figure 3 summarizes our numerical results regarding the propagation of Airy beam in regular photonic lattice as well as positive and negative defects. To get a more detailed insight into this propagation dynamics, we monitor the ratio between the power guided in the central waveguide and the total power of Airy beam as a function of the lattice strength and propagation distance. The numerical results for this power ratio are shown in Fig. 2(a) for a regular lattice, (d) negative defect and (g) positive defect. These graphs clearly demonstrates the impact of optically induced photonic lattice and apropriate defects on the formation of discrete structures, as well as suppression of the acceleration and bending of Airy beam. The Airy beam is launched into the induced photonic lattice with the main lobe exactly located at one lattice site. As the refractive index modulation strength grows, the interaction of Airy beam with lattice sites becomes stronger and consequently the bending of Airy beam is decreased. In the case of regular lattice, for higher refractive index modulations Δn, one can observe the localization of beam power to central waveguide at the back face of crystal. Our results clearly show the slowing down of the self-acceleration of Airy beam (Fig. 3(b),(c)). The corresponding intensity profiles at the back face are indicated with the letters at the respective positions. Depending on the different lattice strengths various kinds of discrete structures arises until the lattice finally suppress the acceleration of Airy beam. Most of the energy then stays in the lattice site, where the main lobe of Airy beam was initially launched.

Then we keep all parameters, but change the refractive index modulation Δn to both, positive and negative defects. The Airy beam is positioned with the main lobe exactly located at the defect site. For the different defects we record the intensity profiles of propagated Airy beam at the back face and monitor the percentage of power guided in the central waveguide, as described previously. Figures 3(d) and 3(g) show the numerical results of power ratio for the negative and

positive defect as a function of the propagation distance and refractive index modulation. The negative defect (Fig. 3(d)) significantly reduces the power guided in defect site and finally repels nearly all power, while the positive defect (Fig. 3(g)) strongly enhances the slowing-down and localization process of Airy beam. Corresponding intensity profiles are shown in the right panel of Fig. 3 for two values of Δn for the negative (e), (f) and positive defect (h), (i).

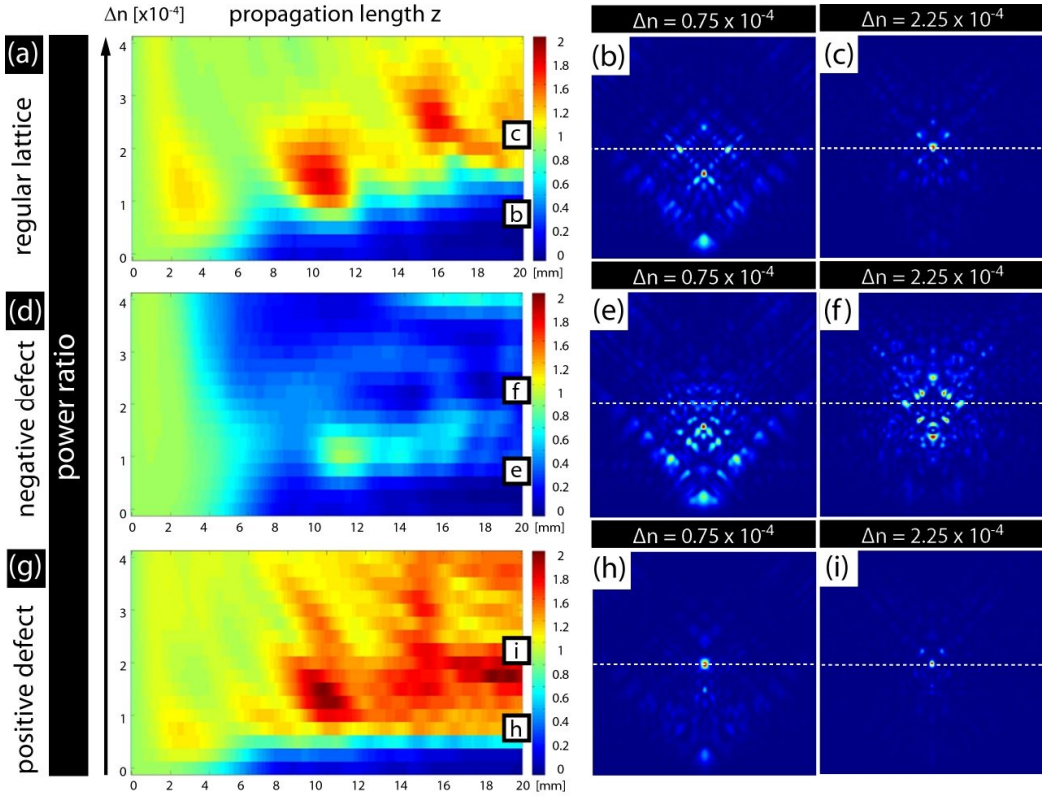

Figure 3. Airy beam propagation in diamond lattice, with and without defects. Dependence of the percentage of Airy beam power in the incident waveguide on refractive index change Δn and propagation length z for a (a) regular lattice, (d) negative defect and (g) positive defect. Numerical results for intensity distributions at the back face for different refractive index change Δn for: (b), (c) regular lattice, (e), (f) negative defect and (h), (i) positive defect.

To experimentally control the index modulation depth we take advantage of the time-dependent build up of induced lattice, which grows monotonously with the writing time. Because in experiments is not possible to record the intensity pattern inside the crystal, we are restricted to the profiles at the back face. In Fig. 4(d) the experimentally measured power ratio at the back face is plotted as a function of the refractive index modulation and defect strength. Therefore, we have repeated the experiments for 11 different defect strengths S_d = -1…1 and recorded the intensity profile at the back face. The modulus of defect strength S_d is given by the ratio of peak intensities of the discrete and the Bessel nondiffracting beam, while the sign is determined by the direction of applied electric field. These results illustrate the strong dependency of propagation and acceleration properties of Airy beam on the lattice depths, as well as the defect strength. The first and third row contains the experimental results – intensity distributions at the back face for two different values of Δn. The corresponding intensity profiles at the back face are indicated with the letters at the respective positions on graph, and presented in: (a), (e) for negative defect, (b), (f) regular lattice and (c), (g) positive defect. The experimental results fully agree with the theoretical analysis. Comparing the numerical intensity distributions of Airy beam at the back phase (Fig. 3) with corresponding experimental results (Fig. 4), one can see a very good qualitative agreement. Also, comparing the numerical graphs for percentage of Airy beam in incident waveguide for propagation distance of 20 mm with experimental graph in Fig. 4(d), very good agreement is observed for defect strength -1, 0 and +1, which corresponds to negative defect, regular lattice and positive defect, respectively.

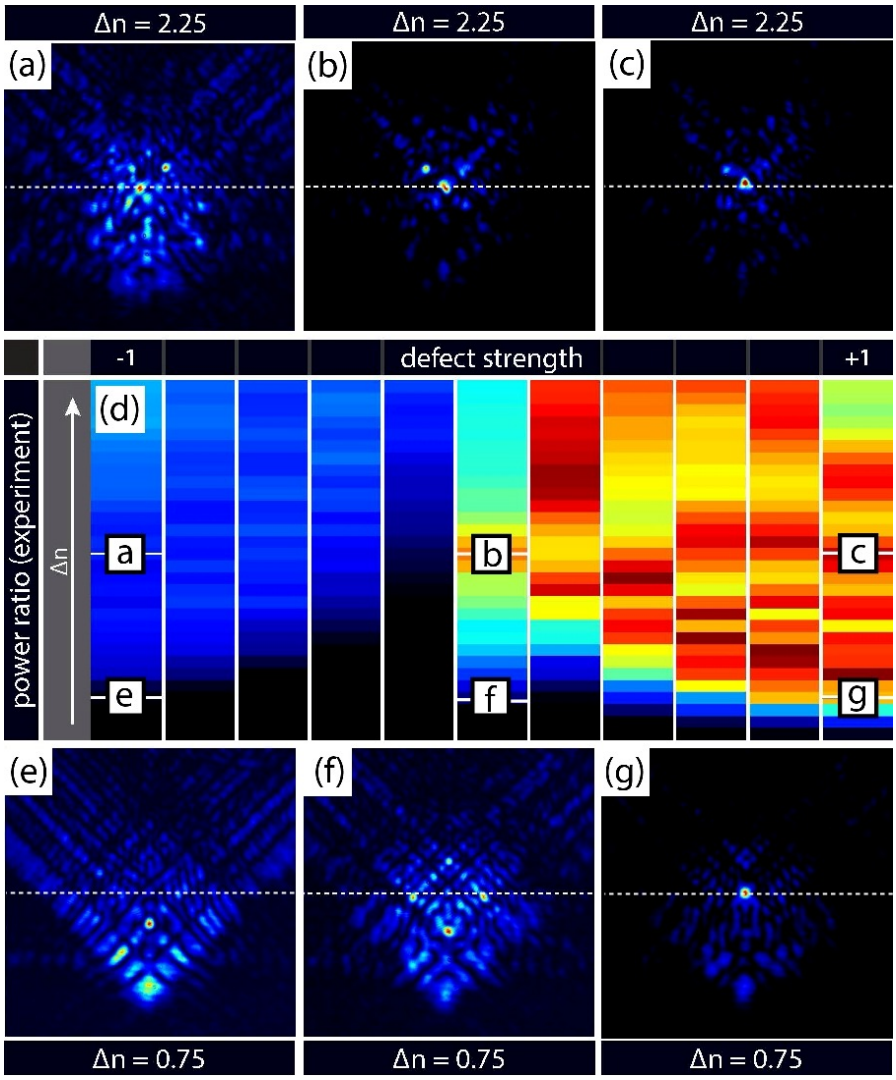

Figure 4. Experimentally observed Airy beam propagation in photonic lattice. (d) Percentage of the Airy beam power propagating in incident waveguide or defect site as a function of refractive index change Δn and defect strength. Exemplary experimental results of Airy beam intensity distribution at the back face for negative defect (a),(e), regular lattice (b),(f) and positive defect(c),(g).

4. CONCLUSIONS

In summary, we have shown, both theoretically and experimentally, that the propagation dynamics of two-dimensional Airy beams could be controlled by optically induced photonic lattices. We demonstrated a way to change the trajectory and shape of finite optical Airy beams. The results depend on the depth of the induced lattice which changes the acceleration and bending of Airy beam. The beam acceleration is slowed down and finally completely stopped for a certain amount of index modulation. Moreover, various single-side defects further affect the beam dynamics as well. By changing the defect strength, as well as the defect type, we can either increase the localization for positive defects, or repel all the power from a defect site, for the negative case. All our presented experimental results fully agree with the supporting numerical simulations.

Acknowledgements

This work is supported by the German Academic Exchange Service (Project 56267010) and Ministry of Education, Science and Technological Development, Republic of Serbia (Project OI 171036).

References

[1] Siviloglou, G. A., Broky, J., Dogariu, A. and Christodoulides, D. N.,"Observation of accelerating Airy beams," Phys. Rev. Lett. 99, 213901 (2007).
[2] Siviloglou, G. A., Broky, J., Dogariu, A. and Christodoulides, D. N., "Self-healing properties of optical Airy beams,"Opt. Lett. 33, 207 (2008).
[3] Baumgartl, J., Mazilu, M. and Dholakia, K., „Optically mediated particle clearing using Airy wavepackets," Nat. Photonics 2, 675–678 (2008).
[4] Polynkin, P., Kolesik, M., Moloney, J. V., Siviloglou, G. A. and Christodoulides, D. N.,"Curved plasma channel generation using ultraintense Airy beams,"Science 324, 229–232 (2009).
[5] Chong, A., Renninger, W. H., Christodoulides, D. N. and Wise, F. W.,"Airy–Bessel wave packets as versatile linear light bullets," Nat. Photonics 4, 103–106 (2010).
[6] Abdollahpour, D., Suntsov, S., Papazoglou, D. G. and Tzortzakis, S.,"Spatiotemporal Airy light bullets in the linear and nonlinear regimes," Phys. Rev. Lett. 105, 253901 (2010).
[7] Kaminer, I., Segev, M., and Christodoulides, D. N.,"Self-accelerating self-trapped optical beams," Phys. Rev. Lett. 106, 213903 (2011).
[8] Ye, Z., Liu, S., Lou, C., Zhang, P., Hu, Y., Song, D., Zhao, J. and Chen, Z., "Acceleration control of Airy beams with optically induced refractive-index gradient," Opt. Lett. 36, 3230 (2011).
[9] Lučić, N. M., Bokić, B. M., Grujić, D. Ž., Pantelić, D. V., Jelenković, B. M., Piper, A., Jović, D. M. and Timotijević, D. V., "Defect-guided Airy beams in optically induced waveguide arrays," Physical Review A 88, 063815(2013).
[10] Terhalle, B., Desyatnikov, A. S., Bersch, C., Träger, D., Tang, L., Imbrock, J., Kivshar, Y. S. and Denz, C., "Anisotropic photonic lattices and discrete solitons in photorefractive media," Applied Physics B 86, 399–405 (2006).
[11] Rose, P., Boguslawski, M. and Denz, C., "Nonlinear lattice structures based on families of complex nondiffracting beams," New Journal of Physics 14, 033018 (2012).
[12] Belić, M. R., Leonardy, J., Timotijević, D. and Kaiser, F., "Spatiotemporal effects in double phase conjugation," Journal of the Optical Society of America B 12, 1602 (1995).
[13] Belić, M., Petrović, M., Jović, D., Strinić, A., Arsenović, D., Motzek, K., Kaiser, F., Jander, P., Denz,C., Tlidi, M. and Mandel, P., "Transverse modulational instabilities of counterpropagating solitons in photorefractive crystals," Optics express 12, 708–16 (2004).
[14] Boguslawski, M., Kelberer, A., Rose, P. and Denz, C., "Multiplexing complex two-dimensional photonic superlattices," Optics Express 20, 27331–43 (2012).